



**HAL**  
open science

## Defects in mucosal immunity and nasopharyngeal dysbiosis in HSC transplanted SCID patients with IL2RG/JAK3 deficiency

Pedro Goncalves, Jean-Marc Doisne, Toshiki Eri, Bruno Charbit, Vincent Bondet, Celine Posseme, Alba Llibre, Consortium The Milieu Interieur, Armanda Casrouge, Christelle Lenoir, et al.

### ► To cite this version:

Pedro Goncalves, Jean-Marc Doisne, Toshiki Eri, Bruno Charbit, Vincent Bondet, et al.. Defects in mucosal immunity and nasopharyngeal dysbiosis in HSC transplanted SCID patients with IL2RG/JAK3 deficiency. *Blood*, 2022, pp.2021014654. 10.1182/blood.2021014654. pasteur-03599568

**HAL Id: pasteur-03599568**

**<https://pasteur.hal.science/pasteur-03599568>**

Submitted on 7 Mar 2022

**HAL** is a multi-disciplinary open access archive for the deposit and dissemination of scientific research documents, whether they are published or not. The documents may come from teaching and research institutions in France or abroad, or from public or private research centers.

L'archive ouverte pluridisciplinaire **HAL**, est destinée au dépôt et à la diffusion de documents scientifiques de niveau recherche, publiés ou non, émanant des établissements d'enseignement et de recherche français ou étrangers, des laboratoires publics ou privés.



Distributed under a Creative Commons Attribution 4.0 International License

## Defects in mucosal immunity and nasopharyngeal dysbiosis in HSC transplanted SCID patients with IL2RG/JAK3 deficiency

Tracking no: BLD-2021-014654R1

Pedro Goncalves (Institut Pasteur, France) Jean-Marc Doisne (Institut Pasteur, France) Toshiki Eri (Institut Pasteur, France) Bruno Charbit (Institut Pasteur, France) Vincent Bondet (Institut Pasteur, France) Celine Posseme (Institut Pasteur, France) Alba Llibre (Institut Pasteur, France) Milieu Interieur Milieu Interieur Consortium (Institut Pasteur, France) Armanda Casrouge (Inserm CIMI U1135, France) Christelle LENOIR (INSERM Unité 1163, France) Bénédicte Neven (Inserm UMR 1163, France) Darragh Duffy (Institut Pasteur, France) Alain Fischer (Inserm UMR 1163, France) James Di Santo (Institut Pasteur, France)

### Abstract:

Both innate and adaptive lymphocytes have critical roles in mucosal defense that contain commensal microbial communities and protect against pathogen invasion. Here we characterize mucosal immunity in human severe combined immunodeficiency (SCID) patients receiving hematopoietic stem cell transplantation (HSCT) with or without myeloablation. We confirmed that pre-transplant conditioning impacted on innate (NK, ILC) and adaptive (B and T cells) lymphocyte reconstitution in these SCID patients and now demonstrate that this further extends to generation of Th2 and Tc2 cells. Using an integrated approach to assess nasopharyngeal immunity, we identify a local mucosal defect in type 2 cytokines, mucus production and a selective local IgA deficiency in HSCT-treated SCID patients with genetic defects in IL2RG/GC or JAK3. These patients have a reduction in IgA-coated nasopharyngeal bacteria and exhibit microbial dysbiosis with increased pathobiont carriage. Interestingly, IVIG replacement therapy can partially normalize nasopharyngeal Ig profiles and restore microbial communities in GC/JAK3 patients. Together, our results suggest a potential non-redundant role for type 2 immunity and/or of local IgA antibody production in the maintenance of nasopharyngeal microbial homeostasis and mucosal barrier function.

**Conflict of interest:** No COI declared

**COI notes:**

**Preprint server:** No;

**Author contributions and disclosures:** P.G. conducted experiments, analyzed the data and prepared the manuscript. J.M.D., T.E., V.B., C.P., A.L., A.C., B.C. performed experiments. C.L. processed samples. D.D. provided logistical support and access to samples from normal individuals via the Milieu Intérieur Consortium. B.N. and A.F. were responsible for patient care, collected samples, designed experiments and prepared the manuscript. J.P.D. designed experiments, analyzed the data, obtained funding, supervised research and prepared the manuscript.

**Non-author contributions and disclosures:** No;

**Agreement to Share Publication-Related Data and Data Sharing Statement:** Data Sharing Statement The raw 16S RNA sequence data for each patient were deposited in the NCBI Sequence Read Archive (SRA) under accession number PRJNA772582. All other datasets generated during the current study are available upon reasonable request via email to the corresponding author.

**Clinical trial registration information (if any):**

1 **Defects in mucosal immunity and nasopharyngeal dysbiosis in HSC**  
2 **transplanted SCID patients with IL2RG/JAK3 deficiency**

3  
4 Pedro Goncalves<sup>1</sup>, Jean-Marc Doisne<sup>1</sup>, Toshiki Eri<sup>1</sup>, Bruno Charbit<sup>2</sup>, Vincent Bondet<sup>3</sup>,  
5 Celine Posseme<sup>3</sup>, Alba Llibre<sup>3</sup>, Milieu Intérieur Consortium<sup>†</sup>, Armanda Casrouge<sup>1</sup>,  
6 Christelle Lenoir<sup>4,5</sup>, Benedicte Neven<sup>4,5,6</sup>, Darragh Duffy<sup>3</sup>, Alain Fischer<sup>4,5,6,7</sup>  
7 and James P. Di Santo<sup>1,\*</sup>

8  
9 <sup>1</sup>Institut Pasteur, Université de Paris, Inserm U1223, Innate Immunity Unit, F-75015  
10 Paris, France

11 <sup>2</sup>Institut Pasteur, Université de Paris, Center for Translational Science, F-75015  
12 Paris, France

13 <sup>3</sup>Institut Pasteur, Université de Paris, Translational Immunology Unit, F-75015 Paris,  
14 France

15 <sup>4</sup>Inserm UMR 1163, F-75015 Paris, France.

16 <sup>5</sup>Université de Paris Descartes Sorbonne Paris Cité, Imagine Institut, F-75015 Paris,  
17 France.

18 <sup>6</sup>Department of Pediatric Immunology, Hematology and Rheumatology, Hôpital  
19 Necker-Enfants Malades, Assistance Publique-Hôpitaux de Paris (APHP), F-75015  
20 Paris, France.

21 <sup>7</sup>Collège de France, F-75231 Paris, France.

22  
23 **\*Corresponding author:** James P. Di Santo, Innate Immunity Unit, Institut Pasteur,  
24 25 Rue du Dr. Roux, 75015 Paris, France; tel: +33-0145688209;  
25 e-mail: [james.di-santo@pasteur.fr](mailto:james.di-santo@pasteur.fr)

26  
27 **Running title:** Type 2 cytokines and IgA promote mucosal immunity

28  
29 **Word count:** 4009 words

30 **Scientific Category:** Immunobiology

31 **Key points:**

- 32 - Pre-transplant conditioning impacts on innate (NK, ILC) and adaptive  
33 lymphocyte reconstitution including the generation of Th2 and Tc2 cells  
34 - GC/JAK3-deficient SCID receiving non-conditioned HSC grafts fail to develop  
35 type 2 responses and have mucosal IgA deficiency with dysbiosis

36 **Abstract**

37

38 Both innate and adaptive lymphocytes have critical roles in mucosal defense that  
39 contain commensal microbial communities and protect against pathogen invasion.  
40 Here we characterize mucosal immunity in human severe combined  
41 immunodeficiency (SCID) patients receiving hematopoietic stem cell transplantation  
42 (HSCT) with or without myeloablation. We confirmed that pre-transplant conditioning  
43 impacted on innate (NK, ILC) and adaptive (B and T cells) lymphocyte reconstitution  
44 in these SCID patients and now demonstrate that this further extends to generation  
45 of Th2 and Tc2 cells. Using an integrated approach to assess nasopharyngeal  
46 immunity, we identify a local mucosal defect in type 2 cytokines, mucus production  
47 and a selective local IgA deficiency in HSCT-treated SCID patients with genetic  
48 defects in IL2RG/GC or JAK3. These patients have a reduction in IgA-coated  
49 nasopharyngeal bacteria and exhibit microbial dysbiosis with increased pathobiont  
50 carriage. Interestingly, IVIG replacement therapy can partially normalize  
51 nasopharyngeal Ig profiles and restore microbial communities in GC/JAK3 patients.  
52 Together, our results suggest a potential non-redundant role for type 2 immunity  
53 and/or of local IgA antibody production in the maintenance of nasopharyngeal  
54 microbial homeostasis and mucosal barrier function.

55

## 56 Introduction

57 Hematopoietic stem cell transplantation (HSCT) for severe combined immune  
58 deficiency (SCID) represents a life-saving therapy for this heterogeneous group of  
59 hematopoietic disorders <sup>1,2</sup>. HSCT generates a variable degree of hematolymphoid  
60 reconstitution that depends on the pre-transplant conditioning regime (eg.  
61 myeloablation) as well as the genetic defect being treated <sup>2,3</sup>. For example, T-B-  
62 natural killer cells (NK)+ SCID resulting from defects in the antigen receptor  
63 recombination pathway harbor immature lymphoid precursors in the thymus and  
64 bone marrow. These patients may receive either myeloablation that can enhance  
65 myeloid and lymphoid reconstitution following HSCT or reduced intensity conditioning  
66 that may eliminate competitive but abnormal thymocyte precursor cells or NK cells. In  
67 contrast, patients with T-B+NK- SCID (caused by mutations in the common  $\gamma$  chain  
68 ( $\gamma$ c) gene *IL2RG* or the Janus kinase *JAK3*) lack lymphoid precursors and are  
69 generally not cytoreduced prior to HSCT <sup>3</sup>. As a result, lymphoid lineages engraft  
70 rapidly but myeloid reconstitution is less robust.

71 Innate lymphoid cells (ILC) are tissue-resident lymphocytes, enriched at  
72 mucosal barriers with roles in immune defense and tissue remodeling <sup>4,5</sup>. Diverse ILC  
73 subsets (ILC1/2/3) produce a restricted range of cytokines that target hematopoietic  
74 as well as non-hematopoietic (stromal, epithelial, endothelial...) cells. <sup>6</sup>. Previous  
75 studies have documented the developmental and functional parallels between ILCs  
76 and T 'helper' (Th) cells <sup>7</sup>. This homology suggests a potential functional redundancy  
77 during immune responses but may also provide a means to synergistically promote  
78 immune defense.

79 Recently it was shown that pre-transplant conditioning allows for better post-  
80 HSCT immune reconstitution with higher frequencies of donor NK and ILC subsets in  
81 myeloablated T-B-NK+ SCID and cancer patients compared with non-conditioned T-  
82 B+NK- SCID recipients <sup>3</sup>. The differential innate lymphoid cell engraftment in these  
83 patients results from a combination of both absence of conditioning and inherent  
84 genetic defects, providing a unique setting (ILC/NK+ versus ILC/NK- phenotypes) to  
85 assess biological roles for ILC/NK cells in human immunity. Interestingly, both HSCT  
86 groups showed robust donor T cell engraftment with restoration of cellular immunity  
87 and recovery of immune competence. In a long-term follow-up of these two HSCT-  
88 treated patient groups, no obvious differences in clinical course or disease  
89 susceptibility were noted. As both HSCT groups showed similar clinical recoveries

90 ('cure'), it was concluded that NK cells and diverse ILC subsets may be redundant for  
91 most aspects of normal human immunity<sup>3,8</sup> that more recently has been extended to  
92 development and function of lymphoid tissues<sup>9</sup>.

93 Diverse ILC subsets are enriched at mucosal surfaces, and in conjunction with  
94 adaptive T and B cell responses, promote barrier defense and tissue regeneration  
95 after infection and inflammation and regulate microbial communities that have a  
96 symbiotic relationship with the host<sup>10,11</sup>. The reciprocal interactions and coordinated  
97 regulation of ILCs versus T helper cells for immune defense remains unclear. A  
98 better characterization of mucosal immunity in ILC/NK+ versus ILC/NK- HSCT  
99 patients may shed light on the specific and/or redundant roles of innate lymphocytes  
100 at barrier surfaces for protection from disease.

101 Here we further analyzed a large cohort of HSCT-treated SCID patients to  
102 assess impact of hematopoietic reconstitution on mucosal barrier function. We  
103 document a selective deficiency in type 2 immunity, strong decreases in  
104 nasopharyngeal IgA and nasal microbial dysbiosis in IL2RG/JAK3-deficient patients  
105 receiving non-conditioned HSCT.

## 106 **Methods**

107

### 108 **Patient and control cohorts**

109 Healthy donors were recruited originally as part of the Milieu Intérieur cohort  
110 (<https://www.milieuinterieur.fr/en/>; Supplementary Materials and Methods). HSCT-  
111 treated SCID patients were followed at Hôpital Necker-Enfants Malades (French  
112 National Reference Center for Primary Immunodeficiencies). Pathogenic mutations  
113 were identified in all cases (Supplementary Table 1). Written informed consent was  
114 obtained from all patients and/or parents. Nasopharyngeal swabs were obtained  
115 concurrently with blood samples during routine visits (no evidence of ongoing  
116 infection, autoimmunity or allergy; no antibiotic use) and were processed as  
117 described<sup>12,13</sup>.

118

### 119 **Cell isolation and FACS analysis**

120 Human peripheral blood mononuclear cells (PBMC) were isolated using density  
121 gradient centrifugation. For FACS analysis, cells were first stained with Flexible  
122 Viability Dye eFluor 506 (eBioscience) following by surface antibodies staining on ice.  
123 Fc receptors were blocked using IgG from human serum (MilliporeSigma). Samples  
124 were acquired with an LSRFortessa (BD) and analyzed by FlowJ10.7.1 (TreeStar).  
125 Bacterial species-specific antibody against microbiota were assessed as described  
126 previous<sup>15</sup>.

127

### 128 **Analysis of nasopharyngeal proteins**

129 Total IgA, IgM, IgG1, IgG2, IgG3 and IgG4 were determined using the Bio-Plex Pro  
130 Human Isotyping Assay Panel (Biorad, Hercules, CA, USA). Data were acquired on a  
131 Bio-Plex 200 System (Bio-Rad) and analyzed with Bio-Plex Manager v5 (Bio-Rad).  
132 IgA1 and IgA2 subclass were measured by Simoa (Quanterix). Total IgD were  
133 determined using a ELISA kit (MBS564048, Mybiosource, San Diego). Total IgE  
134 were determined using a ELISA kit (88-50610, Invitrogen, Massachusetts). Data  
135 were collected with the Multiskan Spectrum (Thermo Fisher Scientific).

136

137 Cytokines were quantified by Simoa® Cytokine 3-Plex B, Discovery or Advantage  
138 Kits (Quanterix) except IFN- $\gamma$  and IL-17F that used Quanterix Homebrew assays.  
139 Nasopharyngeal mucin levels were analyzed using a MUC5AC ELISA Kit (NBP2-

140 76703, Novus Biologicals, diluted 1/50). Eosinophil cationic protein (ECP) were  
141 determined for swabs medium using an ELISA kit (MBS2602477, Mybiosource, San  
142 Diego, USA, diluted 1/2). Total protein content of the supernatants by the Bradford  
143 method <sup>14</sup>.

144

### 145 **16S rRNA sequencing and analysis**

146 16S rRNA sequencing and sequence processing and statistical analysis was  
147 described previous <sup>12,13</sup>. A total of 2.974.329 reads (90.131 reads on average per  
148 sample) was obtained. Raw sequence data have been deposited in the NCBI  
149 Sequence Read Archive (SRA) under accession number (PRJNA772582).

150

### 151 **Bacterial quantification by quantitative RT-PCR assays**

152 Bacterial qPCR used universal 16S rRNA primers to measure total bacteria (16S\_F:  
153 5'-ATTACCGCGGCTGCTGG-3' and 16S and 16S\_R: 5'-ATTACCGCGGCTGCTGG-  
154 3') and *Streptococcus pneumoniae* (*LytA* gene, F: 5'- ACGCAATCTAGCAGATGAAGC-  
155 3' and R: 5'- TGTTTGGTTGGTTATTCGTGC -3').

156

### 157 **Statistical analysis**

158 Statistics were performed using GraphPad Prism (San Diego, USA). P values were  
159 determined by a Kruskal-Wallis test, followed by Dunn's post-test for multiple group  
160 comparisons with median reported; \*P < 0.05; \*\*P < 0.01; \*\*\*P < 0.001. Correlations  
161 between the different assays were calculated using Spearman test. Heatmaps were  
162 generated with Qlucore OMICS explore Version 3.5(26). Correlation matrices were  
163 built using the Spearman correlation and computed using R (v4.0.3).

164



## 165 **Results**

166 This study analyzed a cohort of 21 SCID patients that have been successfully  
167 treated with HSCT at Necker Hospital since 1977. SCID patients with X-linked as well  
168 as autosomal etiologies were included, some patients required Ig replacement  
169 therapy (IgRT) by subcutaneous injection of IgG for specific clinical conditions  
170 (including recurrent respiratory tract infections<sup>16-18</sup>; Supplemental Table 1). Several  
171 patients have been previously reported<sup>3,9</sup>. The group 'GC/JAK3' were T-B+NK- SCID  
172 (IL2RG, JAK3) patients that received non-myeloablative HSCT, and the group 'SCID  
173 other' were T-B-NK+ or T-B+NK+ SCID (RAG1/2, ARTEMIS, MHC Class II, IL7RA)  
174 patients the majority of which received pre-transplant cytoreduction (Supplemental  
175 Table 1). All HSCT-treated SCID patients showed successful donor hematopoietic  
176 reconstitution and recovered T cell immunity. Once clinically stable, patients were  
177 discharged and followed up periodically in our outpatient clinic. The follow up period  
178 varied from 18 to 42 years.

179

### 180 *HSCT-treated GC/JAK3 patients have reduced circulating type 2 lymphocytes*

181 While HSCT-treated SCID patients have stable T cell reconstitution with  
182 balanced CD4/CD8 ratios, naïve T cells and TRECs<sup>1,3,19</sup>, an in-depth analysis of  
183 their differentiated T cell subsets has not been previously performed. ILC and NK cell  
184 reconstitution in SCID patients receiving myeloablative conditioning for HSCT has  
185 only been reported in 2 RAG-deficient patients<sup>3</sup>. As reciprocal interactions between  
186 ILCs and T cells have been documented<sup>20-23</sup>, previously reported lack of NK and  
187 ILCs in the non-conditioned SCID recipients might be associated with perturbations  
188 in their T cell compartment. We paid particular attention to differentiated T cell  
189 subsets that can be identified by expression of specific chemokine receptors (see  
190 Methods; Supplemental Figure 1A, B for FACS gating)<sup>24,25</sup>. Non-conditioned  
191 GC/JAK3 patients receiving IgRT post-HSCT (Supplemental Table 1) were analyzed  
192 separately.

193 Circulating ILCs include CD56+ natural killer (NK) cells (CD56+++CD16- and  
194 CD56+CD16+ cells) and CD127+ ILC2 (CRTH2+) and ILCP (ILC precursors,  
195 CRTH2-CD117+ CD45RA+NKp44-)<sup>26</sup>. Using unsupervised clustering analysis, we  
196 observed a significant reduction in frequencies of NK cells and ILC2 but not ILCP in  
197 GC/JAK3 and GC/JAK3+IgRT patients compared with HC and SCID-other patients  
198 (Figures 1A, B) confirming previous reports in HSCT-treated IL2RG/JAK3-deficient

199 and RAG-deficient patients<sup>3</sup> and further extending this observation to other SCID  
200 etiologies.

201 We next characterized naïve and differentiated CD4<sup>+</sup> T cell subsets in this  
202 SCID cohort. Unsupervised clustering analysis allowed us to identify T cell subsets  
203 including naïve (CD45RA<sup>+</sup>), Treg (CD127<sup>lo</sup>CD25<sup>+</sup>), Tfh (Treg-CD45RA-CXCR5<sup>+</sup>),  
204 Th1 (Treg-CD45RA-CXCR5-CCR6-CXCR3+CCR4<sup>-</sup>), Th2 (Treg-CD45RA-CXCR5-  
205 CCR6-CXCR3-CCR4+CRTH2<sup>+/-</sup>) and Th17 (Treg-CD45RA-CXCR5-CCR6<sup>+</sup>). We  
206 observed a significant reduction in clusters of CCR4+CRTH2<sup>+/-</sup> cells corresponding  
207 to the Th2 subset, as well as a reduction in naïve T cells (CD45RA<sup>+</sup>) in GC/JAK3  
208 and GC/JAK3+IgRT patients compared to HC and SCID-other patients (Figures 1C,  
209 D). Other Th subsets (Th1, Th17, Tfh) were normally present in all HSCT SCID  
210 patients (Figure 1D, Supplemental Figure 2A, B).

211 A similar analysis was performed on CD8<sup>+</sup> T cells. The unsupervised  
212 clustering analysis showed a significant decrease in the CCR4+CRTH2<sup>+</sup> cluster  
213 corresponding to Tc2 subset in CD8<sup>+</sup> T cells in GC/JAK3 and GC/JAK3+IgRT  
214 patients (Figure 1E, F) whereas other CD8<sup>+</sup> T cell subsets were similar in SCID-other  
215 patients as compared to HC (Supplemental Figure 3).

216 The observations of a relative decrease in naïve CD4<sup>+</sup> T cells with a  
217 compensatory increase in activated CD8<sup>+</sup> T cells following HSCT for SCID confirm  
218 earlier work<sup>28</sup>, while our detailed assessment of differentiated T cell subsets allowed  
219 us to identify a selective deficiency in blood CD4<sup>+</sup> Th2 cells and CD8<sup>+</sup> Tc2 cells in  
220 HSCT-treated GC/JAK3 patients. In all SCID etiologies, differentiation of other T  
221 helper subsets (Th1, Th17, Treg) appeared largely intact. These results suggest that  
222 non-conditioned HSCT-treated GC/JAK3 patients manifest a generalized and  
223 selective deficiency in innate and adaptive lymphocytes involved in Type-2 immunity.

224

### 225 *HSCT-treated GC/JAK3 patients have reduced nasopharyngeal type 2 cytokines*

226 We next assessed mucosal immune responses in HSCT-treated SCID  
227 patients. Nasopharyngeal swabs were obtained concurrently with blood samples and  
228 were processed as described<sup>12,13</sup> to yield nucleic acids as well as a soluble fraction  
229 that harbored cytokines, antibodies, anti-microbial peptides and various metabolites.  
230 As differentiated Th cells and ILCs maintain mucosal homeostasis<sup>4,5</sup>, we used digital  
231 ELISA (Simoa) to quantitate cytokines associated with Th1/ILC1, Th2/ILC2 and  
232 Th17/ILC3 responses in these nasopharyngeal samples.

233 We found no significant differences in the levels of type-1 cytokines (IFN- $\gamma$ ,  
234 TNF- $\alpha$ ) in normal controls compared to HSCT-treated GC/JAK3 or SCID-other  
235 patients (Figure 2A). In contrast, levels of type-2 cytokines IL-5 and IL-13 were  
236 clearly decreased in non-conditioned GC/JAK3 patients whereas IL-4 levels were  
237 within healthy ranges (Figure 2B). While the deficiency in nasopharyngeal IL-13  
238 persisted in GC/JAK3 patients receiving IVIG, IL-4 and IL-5 levels were somewhat  
239 higher in these patients compared to non-conditioned GC/JAK3 patients that did not  
240 receive IgRT (Figure 2B). Concerning inflammatory type-3 cytokines (IL-17A, IL-17F,  
241 IL-22), nasopharyngeal mucosal levels were not different from controls except in  
242 GC/JAK3 patients being treated with IgRT (Figure 2C). Whether these increases in  
243 nasopharyngeal cytokines result from IgRT treatment or are related to other  
244 mechanisms that underlie the need to treat (eg. infections) with IgRT is unclear.

245 Type-2 cytokine secretion is regulated by stromal-derived factors and  
246 promotes activation of hematopoietic (eosinophils, mast cells) as well as non-  
247 hematopoietic (goblet cells) targets.<sup>29,30</sup> We found that IL-33 (a major inducer of  
248 recruitment, activation and IL-5 and IL-13 production by type-2 lymphocytes<sup>31-33</sup>)  
249 was not reduced in nasopharyngeal samples (Figure 2D), whereas eosinophil  
250 cationic protein (ECP, marker for tissue eosinophilia<sup>34,35</sup>) was reduced in GC/JAK3  
251 patients consistent with reduced IL-5 levels (Figure 2B, D). Nasopharyngeal IL-6  
252 levels were not significantly elevated in any SCID patient although tended to be  
253 higher in GC/JAK3+IgRT patients (Figure 2D). When all data was clustered, the  
254 heatmap clearly distinguished the defective type-2 cytokine production (in particular,  
255 IL-5 and IL-13) in the context of non-conditioned HSCT for GC/JAK3 and irrespective  
256 of IgRT (Figure 2E).

257

### 258 *Systemic and mucosal Ig subtypes in HSCT-treated SCID patients*

259 Previous studies have analyzed the impact of pre-HCST conditioning on  
260 systemic antibody levels following hematopoietic reconstitution for SCID<sup>18,36</sup>. In  
261 particular, busulfan administration is correlated with higher donor chimerism,  
262 especially in the B cell compartment<sup>36</sup>. We found that non-conditioned GC/JAK3  
263 patients demonstrated somewhat elevated total serum IgM, but all six patients  
264 studied had normal total serum IgG levels (Figure 3A), confirming that GC/JAK3-  
265 deficient B cells can produce switched IgGs in the presence of normal T cells<sup>18</sup>. In  
266 contrast, serum IgA was undetectable (selective IgA deficiency, SIgAD) in half of

267 HSCT-treated GC/JAK3 patients, mirroring previous reports<sup>37,38</sup>. SCID-other patients  
268 harbored normal Ig subtype distributions and levels (Figure 3A). Interestingly, need  
269 for IgRT in GC/JAK3 patients did not clearly correlate with any selective serum Ig  
270 deficiency (Figure 3A) but was dictated by the clinical context (history of recurrent  
271 respiratory tract infections).

272 We next assessed mucosal Igs in HSCT-treated SCID patients by measuring  
273 Ig isotypes and subclasses in paired nasopharyngeal samples. We found that total  
274 nasopharyngeal IgM and IgG was elevated in GC/JAK3 patients compared to  
275 controls but less so compared to SCID-other patients (Figure 3B) which appeared  
276 related to higher levels of IgG3 (Supplemental Figure 4A). In contrast, all GC/JAK3  
277 patients showed a strong reduction in total nasopharyngeal IgA that concomitantly  
278 involved both IgA1 and IgA2 (Figure 3C, Supplemental Figure 4B) and a significant  
279 reduction in total nasopharyngeal IgE (Figure 3D). Interestingly, total nasopharyngeal  
280 IgD levels were significantly increased in GC/JAK3 patients. Lastly, GC/JAK3+IgRT  
281 patients 'normalized' nasopharyngeal Ig distributions with increased IgA and IgE  
282 (Figures 3C, D), although the mechanistic basis remains unclear. Together, our  
283 results demonstrate distinct profiles of systemic and local mucosal IgA responses in  
284 HSCT-treated SCID patients.

285

### 286 *IgG and IgD may provide mucosal protection in the context of IgA deficiency*

287 We next analyzed the binding of different Ig isotypes to nasopharyngeal  
288 microbiota using a flow cytometer-based assay<sup>12</sup>. We found a significant decrease in  
289 the percentage of IgA-coated nasopharyngeal microbes as well as the density of IgA  
290 coating (IgA MFI, not shown) in GC/JAK3 patients compared to SCID-other patients  
291 and healthy controls (Figure 4A, B). Interestingly, GC/JAK3+IgRT patients showed a  
292 partial but significant increase in IgA-coated nasopharyngeal microbes (Figure 4B)  
293 consistent with the increase in nasopharyngeal IgA (Figure 3C). Whether the  
294 increase in IgA activity following IgRT results from an indirect effect following  
295 stimulation of type 2 cytokine production<sup>39-41</sup> remains unclear.

296 Compensatory IgG responses to gut commensal bacterial communities may  
297 operate in the absence of IgA-specific responses<sup>42</sup>. As other Ig isotypes and  
298 subclasses were normally present (IgD) or elevated (IgM, IgG) in GC/JAK3 patients  
299 (Figure 3B), we quantitated the fraction (%) and intensity (MFI) of nasopharyngeal  
300 microbes that were coated with IgG, IgA or IgD using a recently reported multiplexing

301 technique <sup>12</sup>. The majority of nasopharyngeal microbes in healthy individuals are  
302 coated with IgA in combination with IgD and to a lesser extent with IgG (Figure 4C)  
303 <sup>12</sup>. SCID-other patients showed a similar pattern of nasopharyngeal microbe coating,  
304 while nasopharyngeal microbes in GC/JAK3 patients were more abundantly coated  
305 with IgG and IgD alone (Figure 4C). Finally, we observed an increase in IgA/IgG-  
306 double coated nasopharyngeal microbes in GC/JAK3 patients receiving IgRT (Figure  
307 4C), consistent with the increased nasopharyngeal IgA in these individuals. These  
308 results are consistent with the notion that IgG <sup>42</sup> and IgD <sup>43-45</sup> may provide a layer of  
309 mucosal protection during IgA deficiency.

310

### 311 *HSCT-treated GC/JAK3 patients have nasopharyngeal microbiota dysbiosis*

312        Secretory IgA (sIgA) produced locally at mucosal sites plays an essential role  
313 in host defense <sup>12</sup> and shapes commensal microbiota composition and activity in  
314 each individual <sup>46</sup>. To characterize local nasopharyngeal microbial communities, we  
315 performed 16S ribosomal RNA (rRNA) gene sequencing from nasopharyngeal  
316 samples, calculated bacterial beta diversity and subjected sequenced OTU to  
317 Principal Coordinates Analysis (PCoA). We found that nasopharyngeal samples  
318 derived from HSCT-treated GC/JAK3 patients without IVIG replacement therapy  
319 clustered distinctively from the healthy controls and SCID-other patient samples  
320 (Figure 5A) and had elevated beta diversity based on Bray-Curtis, Euclidian and  
321 Jaccard distance matrices (Figure 5B). Accordingly, Shannon and Simpson diversity  
322 indices were reduced in these GC/JAK3 patients (Figure 5C). We further applied a  
323 non-metric multidimensional scaling (NMDS) using Bray-Curtis distances and found a  
324 similar distinctive clustering of GC/JAK3 patients not treated with IVIG  
325 (Supplementary Figure 5A). In contrast, SCID-other patients with more complete  
326 hematopoietic reconstitution showed nasopharyngeal microbial communities that  
327 were more similar to healthy controls (Figures 5A-C, Supplementary Figure 5B).  
328 Total bacterial load was also increased in GC/JAK3 patients not treated with IgRT  
329 compared to healthy controls and other SCID patients (Supplementary Figure 5C).

330        Nasopharyngeal microbial communities in these different SCID patients were  
331 further characterized by annotation of the 16S rRNA datasets. It has been reported  
332 that the nasopharyngeal microbiota of healthy individuals is enriched in commensal  
333 bacteria including *Corynebacterium* and *Dolosigranulum* genera <sup>47,48</sup>. We found a  
334 general reduction in *Dolosigranulum* and *Comamonas* genera in HSCT SCID

335 patients compared to healthy controls and a selective reduction in *Corynebacterium*,  
 336 *Cutibacterium* and *Staphylococcus* genera in GC/JAK3 patients compared to other  
 337 SCID patients and healthy controls (Figure 5D, E). These ‘cornerstone’ bacterial  
 338 communities (particularly *Corynebacterium* and *Dolosigranulum* genera) can reduce  
 339 carriage of several pathobionts (*Streptococcus pneumoniae*, *Haemophilus influenzae*  
 340 and *Moraxella catarrhalis*) that may be present in normal healthy individuals.<sup>49,50</sup>  
 341 Relative abundance of *Streptococcus*, *Haemophilus* and *Moraxella* were not  
 342 significantly increased in HSCT SCID-other patients compared to healthy controls,  
 343 although a higher abundance of *Streptococcus* and *Haemophilus* genera were  
 344 detected in GC/JAK3 patients that were not treated with IgRT (Figure 5D, F). This  
 345 was in part due to the increased abundance of *S. pneumoniae* (Figure 5G;  
 346 Supplementary Figure 5D). Finally, a significant negative correlation of *S.*  
 347 *pneumoniae* abundance with *Dolosigranulum* genus abundance could be detected in  
 348 the nasopharynx (Figure 5H).

349 IgRT is an established treatment to combat infections in HSCT-treated SCID  
 350 patients for which *S. pneumoniae* is a leading cause of disease.<sup>51</sup> Nasopharyngeal  
 351 samples from GC/JAK3 patients receiving IgRT clustered closer to SCID-other  
 352 patients and healthy controls (Figure 5A). Moreover, IgRT in GC/JAK3 patients  
 353 ‘normalized’ microbiota diversity (beta Shannon and Simpson diversity indices) with  
 354 higher representation of *Corynebacterium* and reduced levels of *Streptococcus*  
 355 (Figure 5B-D). Moreover, we could confirm a decrease in *S. pneumoniae* in  
 356 GC/JAK3+IgRT patients (Figure 5G). Intriguingly, IgA level under IgRT correlated  
 357 with microbial  $\alpha$ -diversity indicating the intricate interplay between immune selection  
 358 and maintenance of complex commensal communities (Supplementary Figure 5E).  
 359 Taken together, these data suggest that HSCT-treated GC/JAK3 patients without  
 360 IgRT can present persistent nasopharyngeal microbial dysbiosis with expansion of  
 361 bacteria associated with increased morbidity and mortality risk<sup>51</sup>. As IgRT appears to  
 362 ameliorate the nasopharyngeal dysbiosis, one may consider potential use of IgRT in  
 363 all GC/JAK3 patients to pre-empt or correct this abnormality.

364

365 *Role for type 2 immunity and nasal IgA in maintaining commensal microbiota*  
 366 *diversity and protection against ‘pathobiont’ carriage*

367 Secretory IgA is implicated in human nasopharyngeal microbial homeostasis<sup>52</sup>  
 368 and may protect mucosal surfaces from pathogen invasion through agglutination<sup>53,54</sup>.

369 Still, other 'non-specific' barriers, including a dense mucus layer, restrict commensal  
370 and pathobiont colonization at mucosal sites <sup>55</sup>. While total protein levels in  
371 nasopharyngeal samples from SCID patients and healthy controls were not  
372 significantly different (Supplemental Figure 3B), we found that GC/JAK3 patients  
373 (treated or not with IgRT) had markedly reduced MUC5AC levels compared to SCID-  
374 Other and healthy controls (Figure 6A). MUC5AC levels were positively correlated  
375 with  $\alpha$ -diversity, *Dolosigranulum* and *Corynebacterium* genera abundance and  
376 strongly negatively correlated with *S. pneumoniae* abundance (Figures 6B, C). These  
377 results suggest that nasopharyngeal mucus plays a role in homeostasis of local  
378 commensal microorganisms and is selectively reduced following HSCT for GC/JAK3.

379 We next looked for possible correlations in the cytokine dataset that could  
380 associate with reduced MUC5AC levels in these SCID patients. The reduction in  
381 nasopharyngeal IgA and type 2 cytokine levels in GC/JAK3 patients (Figures 2, 3)  
382 paralleled the observed reductions in MUC5AC (Figure 6D, E), suggesting a possible  
383 link. Type 2 cytokines are known to regulate barrier immunity by promoting mucus  
384 production <sup>29,30</sup> but other factors stimulate epithelial cell renewal and differentiation,  
385 including IL-22 <sup>56</sup>. IL-22 levels were correlated with MUC5AC levels (Supplemental  
386 Figures 6C; see Supplemental Figures 6D for all 2-parameter correlations). Together,  
387 these results identify critical soluble factors that coordinate local mucosal immune  
388 defense in the nasopharynx via mucus production. Finally, a supervised analysis of  
389 nasopharyngeal factors that were significantly different in GC/JAK3 patients reiterate  
390 the key parameters that integrate the unique mucosal immune profile of these  
391 individuals (Figure 6F), including reduced type 2 cytokines, reduced MUC5AC levels,  
392 reduced IgA and microbial dysbiosis.

393

## 394 Discussion

395 In this report, we assess local mucosal immunity in the human nasopharynx in  
396 a well-characterized cohort of SCID patients treated with curative HSCT. Previous  
397 studies on systemic immune reconstitution after BMT have highlighted differences in  
398 homeostasis of peripheral pools of innate and adaptive lymphocytes<sup>1,3,18,19</sup>. Pre-  
399 transplant conditioning regimes may allow for differential engraftment of donor  
400 hematopoietic precursor cells and downstream myeloid and innate lymphocyte pools,  
401 the latter including natural killer (NK) and innate lymphoid cells (ILCs)<sup>3</sup>. The impact  
402 of differences in 'innate reconstitution' on overall systemic immune responses  
403 appeared limited given the similar clinical profiles of these HSCT-treated SCID  
404 patients<sup>3</sup>. These studies raised questions concerning the specific versus redundant  
405 functions of innate lymphocytes in human immunity.

406 As ILCs abundantly populate mucosal sites, we explored their potential  
407 immune roles by comparing HSCT-treated SCID patients that show variable innate  
408 lymphocyte reconstitution<sup>3</sup>. We observed clear differences in mucosal immune  
409 parameters in a subset of SCID patients with genetic defects in GC or JAK3 which  
410 were not conditioned prior to HSCT. We documented a generalized reduction in  
411 mucosal type 2 immunity and IgA production and an inability to maintain 'healthy'  
412 commensal bacterial communities consistent with a defect in nasopharyngeal  
413 mucosal barrier function. In contrast, other SCID etiologies (with or without  
414 myeloablative protocols prior to HSCT) showed normal type 2 cytokines and IgA  
415 production without nasal dysbiosis. Thus the underlying SCID etiology is apparently a  
416 major factor for the observed defects in mucosal immunity.

417 Local IgA production is a hallmark of mucosal immunity and is largely driven  
418 by specific immune responses to resident micro-organisms<sup>57</sup>. Cytokines promote  
419 IgG and IgE production<sup>58</sup>. In contrast, the key soluble factors that regulate switch to  
420 IgA are a matter of debate<sup>57,59</sup>. Previous studies have documented absence of  
421 serum IgA in about half of HSCT-treated GC/JAK3 patients<sup>18,36-38</sup>. Here we show  
422 that mucosal IgA is absent in all HSCT-GC/JAK3 patients examined, including those  
423 with normal circulating IgA. Interestingly, nasopharyngeal type 2 cytokines were most  
424 strongly perturbed in these patients, suggesting a causative link to mucosal IgA  
425 production. Type 2 cytokines can promote the survival and differentiation of tissue  
426 resident memory B cells and IgA secreting plasma cells<sup>60-62,63,64</sup> thereby increasing  
427 IgA production<sup>30,65-68</sup>. Along these lines, a recent report described a major role for



428 ILC2-derived IL-5 in promoting local mucosal IgA production in mice <sup>69</sup>. Whether  
429 locally generated IL-5 (by ILC2 or Th2 cells) regulates mucosal IgA production in  
430 humans remains unclear.

431 An alternative explanation for the observed IgA deficiencies may result from  
432 defective Ig switch in residual GC/JAK3-deficient host B cells, the latter not being  
433 fully replaced by donor HSCT after non-ablative conditioning <sup>36</sup>. The inability of  
434 GC/JAK3-deficient B cells to respond to any  $\gamma_c$ -dependent cytokine might also reduce  
435 IgA switch mechanisms and result in selective IgA deficiency. Still, nasopharyngeal  
436 IgG subclasses were not decreased in HSCT-treated GC/JAK3 patients, and serum  
437 IgG levels were normal consistent with the ability of GC/JAK3-deficient host B cells to  
438 switch Ig isotypes <sup>18</sup>. However, these patients have an intrinsic B cell deficiency  
439 (defective response to IL-2, IL-9 and in part to IL-4) that can affect antibody  
440 production.  $\gamma_c$ -dependent signals in epithelial cells <sup>70</sup> may also play a role. These  
441 observations suggest a contribution of impaired  $\gamma_c$ -dependent signaling pathways to  
442 the defective mucosal IgA production in these patients.

443 Th2 differentiation is considered as a 'default' pathway which can be  
444 subverted to alternative Th fates by environmental signals <sup>71,72</sup>. Still, Th2  
445 differentiation requires reinforcing signals through STAT6 (IL-4, IL-13) to upregulate  
446 GATA3 expression and seal Th2 cell fate <sup>73</sup>. The defect in generation of Th2 cells in  
447 HSCT-treated GC/JAK3 patients may result from the absence of these STAT6-  
448 dependent signals, perhaps delivered by innate lymphocytes (NKT cells, ILC2). In  
449 addition, ILC2 can prime tissue Th2 responses via DC recruitment <sup>20-23</sup>.

450 The mucus layer that lines mucosal surfaces provides a physical barrier to  
451 commensal micro-organisms as well as pathogens and segregates 'niches' harboring  
452 complex microbial biofilms <sup>74</sup>. Secreted mucins (MUC5AC) are produced by goblet  
453 cells in the nasopharyngeal mucosa and tracheobronchial surface epithelium of the  
454 lower respiratory tract that acts as a "scaffold" to present and organize secreted  
455 proteins such as sIgA, antimicrobial peptides (AMPs) and cytokines <sup>74</sup>. Type 2  
456 cytokines (including IL-13) activate goblet cells to produce mucus <sup>29,30</sup>. Whether the  
457 loss of MUC5AC in GC/JAK3 patients secondary to reduced IL-13 predisposes these  
458 individuals to microbial dysbiosis will require further study.

459 Finally, nasopharyngeal IgA deficiency in HSCT-treated GC/JAK3 patients is  
460 associated with local microbial dysbiosis that may have been present prior to HSCT.

461 It is well established that mucosal IgA plays a major role in regulating bacterial  
462 communities in the gut <sup>46,75</sup> and the reduction in nasopharyngeal IgA observed in  
463 GC/JAK3 patients is correlated with loss of microbial diversity and frequently  
464 accompanied by increased pathobiont carriage. While other Ig subclasses are  
465 present (and even elevated) in the nasopharynx in these patients and are able to  
466 coat bacteria, IgA remains a non-redundant immune factor required for microbial  
467 mucosal homeostasis.

## 468 **Acknowledgments**

469 We thank Sean Kennedy and Laurence Motreff (Biomics Platform) for 16S rRNA  
470 sequencing, Amine Ghozlane and Emna Achouri (HUB) for assistance with  
471 sequencing data analysis and the Di Santo laboratory for discussions. This study was  
472 supported by grants from the Institut Pasteur, INSERM, ANR (15-CE15-000-  
473 ILC3\_MEMORY) and ERC (695467-ILC\_REACTIVITY). P. Gonçalves was supported  
474 in part by the Labex Milieu Intérieur (ANR 10-LBX-69 MI). The Biomics Platform is  
475 supported by France Génomique (ANR-10-INBS-09-09) and IBISA.  
476

477

## 478 **Contributions**

479 P.G. conducted experiments, analyzed the data and prepared the manuscript.  
480 J.M.D., T.E., V.B., C.P., A.L., A.C., B.C. performed experiments. C.L. processed  
481 samples. D.D. provided logistical support and access to samples from normal  
482 individuals via the Milieu Intérieur Consortium. B.N. and A.F. were responsible for  
483 patient care, collected samples, designed experiments and prepared the manuscript.  
484 J.P.D. designed experiments, analyzed the data, obtained funding, supervised  
485 research and prepared the manuscript.

486

## 487 **Competing interests**

488 The authors declare no competing interests.

489

## 490 **Data Sharing Statement**

491 The raw 16S RNA sequence data were deposited in the NCBI Sequence Read  
492 Archive (SRA) under accession number PRJNA772582. All other datasets generated

493 during the current study are available upon reasonable request via email to the  
494 corresponding author.

495

496

497 **References**

- 498 1. Neven B, Leroy S, Decaluwe H, et al. Long-term outcome after hematopoietic  
499 stem cell transplantation of a single-center cohort of 90 patients with severe  
500 combined immunodeficiency. *Blood*. 2009;113(17):4114-4124.
- 501 2. Castagnoli R, Delmonte OM, Calzoni E, Notarangelo LD. Hematopoietic Stem Cell  
502 Transplantation in Primary Immunodeficiency Diseases: Current Status and Future  
503 Perspectives. *Frontiers in Pediatrics*. 2019;7:295.
- 504 3. Vely F, Barlogis V, Vallentin B, et al. Evidence of innate lymphoid cell redundancy  
505 in humans. *Nature Immunology*. 2016;17(11):1291-1299.
- 506 4. Bal SM, Bernink JH, Nagasawa M, et al. IL-1beta, IL-4 and IL-12 control the fate of  
507 group 2 innate lymphoid cells in human airway inflammation in the lungs. *Nature*  
508 *Immunology*. 2016;17(6):636-645.
- 509 5. Simoni Y, Fehlings M, Klooverpris HN, et al. Human Innate Lymphoid Cell Subsets  
510 Possess Tissue-Type Based Heterogeneity in Phenotype and Frequency (vol 46, pg  
511 148, 2017). *Immunity*. 2018;48(5):1060-1060.
- 512 6. Vivier E, Artis D, Colonna M, et al. Innate Lymphoid Cells: 10 Years On. *Cell*.  
513 2018;174(5):1054-1066.
- 514 7. Cherrier DE, Serafini N, Di Santo JP. Innate Lymphoid Cell Development: A T Cell  
515 Perspective. *Immunity*. 2018;48(6):1091-1103.
- 516 8. Fischer A, Rausell A. Primary immunodeficiencies suggest redundancy within the  
517 human immune system. *Science Immunology*. 2016;1(6):eaah5861.
- 518 9. Berteloot L, Molina TJ, Bruneau J, et al. Alternative pathways for the development  
519 of lymphoid structures in humans. *Proceedings of the National Academy of Sciences*  
520 *of the United States of America*. 2021;118(29):e2108082118.
- 521 10. Thibeault C, Suttorp N, Opitz B. The microbiota in pneumonia: From protection to  
522 predisposition. *Science Translational Medicine*. 2021;13(576):eaba0501.
- 523 11. Hooper LV, Littman DR, Macpherson AJ. Interactions Between the Microbiota  
524 and the Immune System. *Science*. 2012;336(6086):1268-1273.
- 525 12. Goncalves P, Charbit B, Lenoir C, et al. Antibody-coated microbiota in  
526 nasopharynx of healthy individuals and hypogammaglobulinemia patients. *J Allergy*  
527 *Clin Immunol*. 2020; 145(6):1686-1690.
- 528 13. Smith N, Goncalves P, Charbit B, et al. Distinct systemic and mucosal immune  
529 responses during acute SARS-CoV-2 infection. *Nature Immunology*. 2021;  
530 22(11):1428-1439.

- 531 14. Bradford MM. A rapid and sensitive method for the quantitation of microgram  
532 quantities of protein utilizing the principle of protein-dye binding. *Anal Biochem.*  
533 1976;72:248-254.
- 534 15. Moor K, Fadlallah J, Toska A, et al. Analysis of bacterial-surface-specific  
535 antibodies in body fluids using bacterial flow cytometry. *Nature Protocols.*  
536 2016;11(8):1531-1553.
- 537 16. Buckley RH, Schiff SE, Schiff RI, et al. Hematopoietic stem-cell transplantation  
538 for the treatment of severe combined immunodeficiency. *N Engl J Med.*  
539 1999;340(7):508-516.
- 540 17. Haddad E, Landais P, Friedrich W, et al. Long-term immune reconstitution and  
541 outcome after HLA-nonidentical T-cell-depleted bone marrow transplantation for  
542 severe combined immunodeficiency: a European retrospective study of 116 patients.  
543 *Blood.* 1998;91(10):3646-3653.
- 544 18. Haddad E, Le Deist F, Aucouturier P, et al. Long-term chimerism and B-cell  
545 function after bone marrow transplantation in patients with severe combined  
546 immunodeficiency with B cells: A single-center study of 22 patients. *Blood.*  
547 1999;94(8):2923-2930.
- 548 19. Borghans JA, Bredius RG, Hazenberg MD, et al. Early determinants of long-term  
549 T-cell reconstitution after hematopoietic stem cell transplantation for severe  
550 combined immunodeficiency. *Blood.* 2006;108(2):763-769.
- 551 20. Oliphant CJ, Hwang YY, Walker JA, et al. MHCII-Mediated Dialog between  
552 Group 2 Innate Lymphoid Cells and CD4(+) T Cells Potentiates Type 2 Immunity and  
553 Promotes Parasitic Helminth Expulsion. *Immunity.* 2014;41(2):283-295.
- 554 21. Gold MJ, Antignano F, Halim TYF, et al. Group 2 innate lymphoid cells facilitate  
555 sensitization to local, but not systemic, T(H)2-einducing allergen exposures. *Journal*  
556 *of Allergy and Clinical Immunology.* 2014;133(4):1142-1148.
- 557 22. Halim TYF, Rana BMJ, Walker JA, et al. Tissue-Restricted Adaptive Type 2  
558 Immunity Is Orchestrated by Expression of the Costimulatory Molecule OX40L on  
559 Group 2 Innate Lymphoid Cells. *Immunity.* 2018;48(6):1195-1207.
- 560 23. Min J, Li Z, Wang J, Zhang F, Li F, Ding J. ILC2s induces adaptive Th2-type  
561 immunity in acute exacerbation of chronic obstructive pulmonary disease. *European*  
562 *Journal of Immunology.* 2019;49:445-446.
- 563 24. Gaylo-Moynihan A, Prizant H, Popovic M, et al. Programming of Distinct  
564 Chemokine-Dependent and -Independent Search Strategies for Th1 and Th2 Cells  
565 Optimizes Function at Inflamed Sites. *Immunity.* 2019;51(2):298-309.
- 566 25. Morita R, Schmitt N, Bentebibel SE, et al. Human Blood CXCR5(+)CD4(+) T  
567 Cells Are Counterparts of T Follicular Cells and Contain Specific Subsets that  
568 Differentially Support Antibody Secretion. *Immunity.* 2011;34(1):135-135.

- 569 26. Lim AI, Li Y, Lopez-Lastra S, et al. Systemic Human ILC Precursors Provide a  
570 Substrate for Tissue ILC Differentiation. *Cell*. 2017;168(6):1086-1100.
- 571 27. van Unen V, Holtt T, Pezzotti N, et al. Visual analysis of mass cytometry data by  
572 hierarchical stochastic neighbour embedding reveals rare cell types. *Nature*  
573 *Communications*. 2017;8(1):1740.
- 574 28. Sarzotti M, Patel DA, Li XJ, et al. T cell repertoire development in humans with  
575 SCID after nonablative allogeneic marrow transplantation. *Journal of Immunology*.  
576 2003;170(5):2711-2718.
- 577 29. Wynn TA. Fibrotic disease and the T(H)1/T(H)2 paradigm. *Nat Rev Immunol*.  
578 2004;4(8):583-594.
- 579 30. Moro K, Yamada T, Tanabe M, et al. Innate production of T(H)2 cytokines by  
580 adipose tissue-associated c-Kit(+)Sca-1(+) lymphoid cells. *Nature*.  
581 2010;463(7280):540-544.
- 582 31. Puttur F, Denney L, Gregory LG, et al. Pulmonary environmental cues drive  
583 group 2 innate lymphoid cell dynamics in mice and humans. *Science Immunology*.  
584 2019;4(36):eaav7638.
- 585 32. Salimi M, Barlow JL, Saunders SP, et al. A role for IL-25 and IL-33-driven type-2  
586 innate lymphoid cells in atopic dermatitis. *J Exp Med*. 2013;210(13):2939-2950.
- 587 33. Stier MT, Zhang J, Goleniewska K, et al. IL-33 promotes the egress of group 2  
588 innate lymphoid cells from the bone marrow. *Journal of Experimental Medicine*.  
589 2018;215(1):263-281.
- 590 34. Nussbaum JC, Van Dyken SJ, von Moltke J, et al. Type 2 innate lymphoid cells  
591 control eosinophil homeostasis. *Nature*. 2013;502(7470):245-248.
- 592 35. Nahm DH, Park HS. Correlation between IgA antibody and eosinophil cationic  
593 protein levels in induced sputum from asthmatic patients. *Clinical and Experimental*  
594 *Allergy*. 1997;27(6):676-681.
- 595 36. Miggelbrink AM, Logan BR, Buckley RH, et al. B cell differentiation and IL-21  
596 response in IL2RG/JAK3 SCID patients after hematopoietic stem cell transplantation.  
597 *Blood*. 2018;131(26):2967-2977.
- 598 37. Buckley RH, Schiff SE, Sampson HA, et al. Development of Immunity in Human  
599 Severe Primary T-Cell Deficiency Following Haploidentical Bone-Marrow Stem-Cell  
600 Transplantation. *Journal of Immunology*. 1986;136(7):2398-2407.
- 601 38. Buckley RH, Win CM, Moser BK, Parrott RE, Sajaroff E, Sarzotti-Kelsoe M. Post-  
602 Transplantation B Cell Function in Different Molecular Types of SCID. *Journal of*  
603 *Clinical Immunology*. 2013;33(1):96-110.

- 604 39. Anthony RM, Kobayashi T, Wermeling F, Ravetch JV. Intravenous  
605 gammaglobulin suppresses inflammation through a novel T(H)2 pathway. *Nature*.  
606 2011;475(7354):110-113.
- 607 40. Tjon ASW, van Gent R, Jaadar H, et al. Intravenous Immunoglobulin Treatment  
608 in Humans Suppresses Dendritic Cell Function via Stimulation of IL-4 and IL-13  
609 Production. *Journal of Immunology*. 2014;192(12):5625-5634.
- 610 41. Kazatchkine MD, Kaveri SV. Advances in immunology: Immunomodulation of  
611 autoimmune and inflammatory diseases with intravenous immune globulin. *New*  
612 *England Journal of Medicine*. 2001;345(10):747-755.
- 613 42. Fadlallah J, Sterlin D, Fieschi C, et al. Synergistic convergence of microbiota-  
614 specific systemic IgG and secretory IgA. *J Allergy Clin Immunol*. 2019;143(4):1575-  
615 1585.
- 616 43. Chen K, Cerutti A. New insights into the enigma of immunoglobulin D.  
617 *Immunological Reviews*. 2010;237(1):160-179.
- 618 44. Chen K, Xu W, Wilson M, et al. Immunoglobulin D enhances immune surveillance  
619 by activating antimicrobial, proinflammatory and B cell-stimulating programs in  
620 basophils. *Nat Immunol*. 2009;10(8):889-898.
- 621 45. Forsgren A, Brant M, Mollenkvist A, et al. Isolation and characterization of a novel  
622 IgD-binding protein from *Moraxella catarrhalis*. *Journal of Immunology*.  
623 2001;167(4):2112-2120.
- 624 46. Fadlallah J, El Kafsi H, Sterlin D, et al. Microbial ecology perturbation in human  
625 IgA deficiency. *Sci Transl Med*. 2018;10(439):eaan1217.
- 626 47. Piters WAAD, Jochems SP, Mitsi E, et al. Interaction between the nasal  
627 microbiota and *S.pneumoniae* in the context of live-attenuated influenza vaccine.  
628 *Nature Communications*. 2019;10(1):2981.
- 629 48. Kelly MS, Surette MG, Smieja M, et al. The Nasopharyngeal Microbiota of  
630 Children With Respiratory Infections in Botswana. *Pediatric Infectious Disease*  
631 *Journal*. 2017;36(9):E211-E218.
- 632 49. Brugger SD, Bomar L, Lemon KP. Commensal-Pathogen Interactions along the  
633 Human Nasal Passages. *Plos Pathogens*. 2016;12(7):e1005633.
- 634 50. Bomar L, Brugger SD, Yost BH, Davies SS, Lemon KP. *Corynebacterium*  
635 *accolens* Releases Antipneumococcal Free Fatty Acids from Human Nostril and Skin  
636 Surface Triacylglycerols. *Mbio*. 2016;7(1):e01725-15.
- 637 51. Engelhard D, Cordonnier C, Shaw PJ, et al. Early and late invasive  
638 pneumococcal infection following stem cell transplantation: a European Bone Marrow  
639 Transplantation survey. *British Journal of Haematology*. 2002;117(2):444-450.



- 640 52. Bunker JJ, Erickson SA, Flynn TM, et al. Natural polyreactive IgA antibodies coat  
641 the intestinal microbiota. *Science*. 2017;358(6361):eaan6619.
- 642 53. Binsker U, Lees JA, Hammond AJ, Weiser JN. Immune exclusion by naturally-  
643 acquired secretory IgA to the pneumococcal pilus-1. *J Clin Invest*. 2019;130(2):927-  
644 941.
- 645 54. Roche AM, Richard AL, Rahkola JT, Janoff EN, Weiser JN. Antibody blocks  
646 acquisition of bacterial colonization through agglutination. *Mucosal Immunology*.  
647 2015;8(1):176-185.
- 648 55. Ha U, Lim JH, Jono H, et al. A novel role for I kappa B kinase (IKK) alpha and  
649 IKK beta in ERK-dependent up-regulation of MUC5AC mucin transcription by  
650 *Streptococcus pneumoniae*. *Journal of Immunology*. 2007;178(3):1736-1747.
- 651 56. Fujisawa T, Velichko S, Thai P, Hung LY, Huang F, Wu R. Regulation of Airway  
652 MUC5AC Expression by IL-1 beta and IL-17A; the NF-kappa B Paradigm. *Journal of*  
653 *Immunology*. 2009;183(10):6236-6243.
- 654 57. Bunker JJ, Bendelac A. IgA Responses to Microbiota. *Immunity*. 2018;49(2):211-  
655 224.
- 656 58. Snapper CM, Finkelman FD, Paul WE. Regulation of Igg1 and Ige Production by  
657 Interleukin-4. *Immunological Reviews*. 1988;102:51-75.
- 658 59. Cerutti A. The regulation of IgA class switching. *Nature Reviews Immunology*.  
659 2008;8(6):421-434.
- 660 60. Scheeren FA, Naspetti M, Diehl S, et al. STAT5 regulates the self-renewal  
661 capacity and differentiation of human memory B cells and controls Bcl-6 expression.  
662 *Nature Immunology*. 2005;6(3):303-313.
- 663 61. Malin S, McManus S, Cobaleda C, et al. Role of STAT5 in controlling cell survival  
664 and immunoglobulin gene recombination during pro-B cell development. *Nat*  
665 *Immunol*. 2010;11(2):171-179.
- 666 62. Diehl SA, Schmidlin H, Nagasawa M, et al. STAT3-mediated up-regulation of  
667 BLIMP1 is coordinated with BCL6 down-regulation to control human plasma cell  
668 differentiation. *Journal of Immunology*. 2008;180(7):4805-4815.
- 669 63. Matsumoto R, Matsumoto M, Mita S, et al. Interleukin-5 Induces Maturation but  
670 Not Class Switching of Surface Iga-Positive-B Cells into Iga-Secreting Cells.  
671 *Immunology*. 1989;66(1):32-38.
- 672 64. Karasuyama H, Rolink A, Melchers F. Recombinant Interleukin-2 or Interleukin-5,  
673 but Not Interleukin-3 or Interleukin-4, Induces Maturation of Resting Mouse  
674 Lymphocytes-B and Propagates Proliferation of Activated B-Cell Blasts. *Journal of*  
675 *Experimental Medicine*. 1988;167(4):1377-1390.

- 676 65. Drake LY, Iijima K, Bartemes K, Kita H. Group 2 Innate Lymphoid Cells Promote  
677 an Early Antibody Response to a Respiratory Antigen in Mice. *Journal of*  
678 *Immunology*. 2016;197(4):1335-1342.
- 679 66. Fort MM, Cheung J, Yen D, et al. IL-25 induces IL-4, IL-5, and IL-13 and Th2-  
680 associated pathologies in vivo. *Immunity*. 2001;15(6):985-995.
- 681 67. Moon BG, Takaki S, Miyake K, Takatsu K. The role of IL-5 for mature B-1 cells in  
682 homeostatic proliferation, cell survival, and Ig production. *Journal of Immunology*.  
683 2004;172(10):6020-6029.
- 684 68. Beagley KW, Eldridge JH, Kiyono H, et al. Recombinant murine IL-5 induces high  
685 rate IgA synthesis in cycling IgA-positive Peyer's patch B cells. *J Immunol*.  
686 1988;141(6):2035-2042.
- 687 69. Satoh-Takayama N, Kato T, Motomura Y, et al. Bacteria-Induced Group 2 Innate  
688 Lymphoid Cells in the Stomach Provide Immune Protection through Induction of IgA.  
689 *Immunity*. 2020;52(4):635-649.
- 690 70. Laffort C, Le Deist F, Favre M, Caillat-Zucman S, Radford-Weiss I, Debré M,  
691 Freitag S, Blanche S, Cavazzana-Calvo M, de Saint Basile G, de Villartay JP, Giliani  
692 S, Orth G, Casanova JL, Bodemer C, Fischer A. Severe cutaneous papillomavirus  
693 disease after haemopoietic stem-cell transplantation in patients with severe  
694 combined immune deficiency caused by common gamma cytokine receptor subunit  
695 or JAK-3 deficiency. *Lancet*. 2004 Jun 19;363(9426):2051-4.
- 696 71. Gieseck RL, Wilson MS, Wynn TA. Type 2 immunity in tissue repair and fibrosis.  
697 *Nature Reviews Immunology*. 2018;18(1):62-76.
- 698 72. Lloyd CM, Snelgrove RJ. Type 2 immunity: Expanding our view. *Science*  
699 *Immunology*. 2018;3(25):eaat1604.
- 700 73. Zhu JF, Guo LY, Watson CJ, Hu-Li J, Paul WE. Stat6 is necessary and sufficient  
701 for IL-4's role in Th2 differentiation and cell expansion. *Journal of Immunology*.  
702 2001;166(12):7276-7281.
- 703 74. Zanin M, Baviskar P, Webster R, Webby R. The Interaction between Respiratory  
704 Pathogens and Mucus. *Cell Host & Microbe*. 2016;19(2):159-168.
- 705 75. Sterlin D, Fadlallah J, Adams O, et al. Human IgA bind a diverse array of  
706 commensal bacteria. *Journal of Experimental Medicine*. 2020;217(3):e20181635.  
707

708 **Figure Legends**

709

710 **Figure 1. FACS analysis of peripheral blood mononuclear cells (PBMCs)**  
 711 **reveal a defect in differentiation of type-2 lymphocytes in HSCT-treated**  
 712 **GC/JAK3 patients. A,** Unsupervised Uniform Manifold Approximation and  
 713 Projection (UMAP)<sup>27</sup> of single live CD45+Lin-CD3-CD4-CD7+ cells was applied for  
 714 CD56, CD16, CD94, NKp46, CD94, CD127, CD161, CD25, CD117 and CRTH2  
 715 fluorescence parameters. **B,** Supervised analysis of circulating innate lymphoid cells  
 716 (ILCs) including two CD56+ subsets of natural killer (NK) cells and two CD127+  
 717 subsets denoted as ILC2 (CRTh2+) and ILCP (ILC precursors, CRTh2-  
 718 CD117+CD45RA+NKp44-) (manually gating strategy on Supplemental Figure 1A). **C,**  
 719 UMAP analysis on CD4+ T cells including CXCR3, CCR4, CRTH2, CCR6, CXCR5,  
 720 CD25, CD127 and CD45RA fluorescence parameters (Supplemental Figure 2A). **D,**  
 721 Supervised analysis of circulating T cell populations. The different subsets were  
 722 identified as follow: Naïve (CD45RA+), Th1 (Treg-CD45RA-CXCR5-CCR6-  
 723 CXCR3+CCR4-), Th17 (Treg-CD45RA-CXCR5-CCR6+), Th2 (Treg-CD45RA-  
 724 CXCR5-CCR6-CXCR3-CCR4+CRTH2+/-) and Treg (CD127loCD25+) (manually  
 725 gating strategy on Supplemental Figure 1B). **E,** UMAP analysis on CD8+ Tc2 subset  
 726 including CCR4 and CRTH2 fluorescence parameters (Supplemental Figure 3). **F,**  
 727 Supervised analysis of circulating CD8+ Tc2 subset defined as CD45RA-CD25-  
 728 CD94-CD56-CXCR5-CCR6-CXCR3-CCR4+CRTH2+/- . In **(B)**, **(D)** and **(F)**, box plots  
 729 with median ± minimum to maximum. P values were determined with the Kruskal  
 730 Wallis test followed by with Dunn's post test for multiple group comparisons; \*P <  
 731 0.05, \*\*P < 0.005, \*\*\*P < 0.001.

732

733 **Figure 2. HSCT-treated GC/JAK3 patients have a generalized defect in**  
 734 **nasopharyngeal type 2 immunity. A,** Nasopharyngeal levels of type 1 cytokines  
 735 (IFN-γ and TNF-α). **B,** Nasopharyngeal levels of type 2 cytokines (IL-4, IL-5 and IL-  
 736 13). **C,** Nasopharyngeal levels of type 3 cytokines (IL-17A, IL-17F and IL-22). **D,**  
 737 Nasopharyngeal levels of IL-33, IL-6 and Eosinophil cationic protein (ECP)/RNase 3.  
 738 **E,** Heatmap representation of the mean of the concentration of all nasopharyngeal  
 739 cytokines in healthy and HSCT-treated SCID patients. In **(A)**, **(B)**, **(C)**, and **(D)**, box  
 740 plots with median ± minimum to maximum. P values were determined with the

741 Kruskal Wallis test followed by with Dunn's post test for multiple group comparisons;  
 742 \*P < 0.05, \*\*P < 0.005, \*\*\*P < 0.001.

743

744 **Figure 3. HSCT-treated GC/JAK3 patients without Igs replacement therapy**  
 745 **have decrease in nasopharyngeal secretory IgA (SIgA).** **A,** Serum Igs  
 746 concentration in healthy and HSCT-treated SCID patients. **B,** Nasopharyngeal  
 747 concentrations of total IgM, IgD and IgG in healthy and HSCT-treated SCID patients.  
 748 **C,** Nasopharyngeal concentrations of total IgA and IgA1 and IgA2 in healthy and  
 749 HSCT-treated SCID patients. **D,** Nasopharyngeal concentrations of total IgE in  
 750 healthy and HSCT-treated SCID patients. In **(A), (B), (C),** and **(D),** box plots with  
 751 median  $\pm$  minimum to maximum. P values were determined with the Kruskal Wallis  
 752 test followed by with Dunn's post test for multiple group comparisons; \*P < 0.05, \*\*P  
 753 < 0.005, \*\*\*P < 0.001.

754

755 **Figure 4. HSCT-treated GC/JAK3 patients without IVIG replacement therapy**  
 756 **have decreased IgA-coating of nasopharyngeal bacteria.** **A,** Representative dot  
 757 plots of IgA, IgG and IgD binding to nasopharyngeal microbiota in healthy and HSCT-  
 758 treated SCID patients. **B,** % of IgA/IgG/IgD coated nasopharynx microbes in healthy  
 759 and HSCT-treated SCID patients. **C,** Double IgA/IgG or IgA/IgD coated nasopharynx  
 760 microbes in healthy and HSCT-treated SCID patients. In **(A), (B), (C),** box plots with  
 761 median  $\pm$  minimum to maximum. P values were determined with the Kruskal Wallis  
 762 test followed by with Dunn's post test for multiple group comparisons; \*P < 0.05, \*\*P  
 763 < 0.005, \*\*\*P < 0.001.

764

765 **Figure 5. HSCT-treated GC/JAK3 patients without IVIG replacement therapy**  
 766 **have nasopharyngeal microbiota dysbiosis.** **A,** Unsupervised principal coordinate  
 767 analysis (PCoA) of 16S RNA sequencing Operational Taxonomic Units (OTU) of the  
 768 healthy controls and HSCT-treated SCID patients along the first two principal  
 769 coordinate (PC) axes, based on Bray-Curtis distances. The respective PERMANOVA  
 770 test showing that nasopharynx microbiota from SCIDX/JAK3 patients is significantly  
 771 different from healthy controls. **B,** The beta ( $\beta$ ) diversity, calculated using the Bray-  
 772 Curtis, Jaccard and Euclidean distances, among subjects by group. **C,** The alpha ( $\alpha$ )  
 773 diversity, calculated using the Shannon index and Simpson index in healthy and  
 774 HSCT-treated SCID patients. Mean and standard error of mean (SEM) values are

775 indicated. **D**, Bar plot showing the mean of the microbiota Genus abundance (%) in  
 776 healthy and HSCT-treated SCID patients. **(E)** and **(F)** Individual Genus abundance  
 777 (%) plots in healthy and HSCT-treated SCID patients. **G**, Individual *Streptococcus*  
 778 *pneumoniae* (%) plot in healthy and HSCT-treated SCID patients. **H**, show individual  
 779 correlation plot between *Streptococcus* Genus abundance (%) and *Dolosigranalum*  
 780 Genus abundance (%). In **(B)**, **(E)**, **(F)** and **(G)** box plots with median  $\pm$  minimum to  
 781 maximum. P values were determined with the Kruskal Wallis test followed by with  
 782 Dunn's post test for multiple group comparisons; \*P < 0.05, \*\*P < 0.005, \*\*\*P <  
 783 0.001. In **(H)**,  $\sigma$  represents Spearman coefficient and p the p value.

784

785 **Figure 6. Defective type 2 immunity underlies nasopharyngeal dysbiosis in**  
 786 **HSCT-treated GC/JAK3 patients. A**, Nasopharyngeal MUC5AC concentration in  
 787 healthy and HSCT-treated SCID patients. **B**, Individual correlation plot between  
 788 nasopharyngeal MUC5AC concentration and  $\alpha$ -diversity. **C**, Individual correlation plot  
 789 between nasopharyngeal MUC5AC concentration and *Dolosigranalum* genus  
 790 abundance (%) or *Streptococcus pneumoniae* abundance (%). **D**, Individual  
 791 correlation plot between nasopharyngeal MUC5AC concentration and  
 792 nasopharyngeal IL-4, IL-5, and IL-13 concentration. **E**, Individual correlation plot  
 793 between nasopharyngeal MUC5AC concentration and nasopharyngeal secretory IgA  
 794 (SIgA). **F**, Heatmap representation of statistically different (P<0.05) nasopharyngeal  
 795 features between GC/JAK3 patients and the other patients and the 3D PcoA  
 796 representation. In **(A)** box plots with median  $\pm$  minimum to maximum. P values were  
 797 determined with the Kruskal Wallis test followed by with Dunn's post test for multiple  
 798 group comparisons; \*P < 0.05, \*\*P < 0.005. In **(B)**, **(C)**, **(D)** and **(E)**  $\sigma$  represents  
 799 Spearman coefficient and p the p value.

**Figure 1**

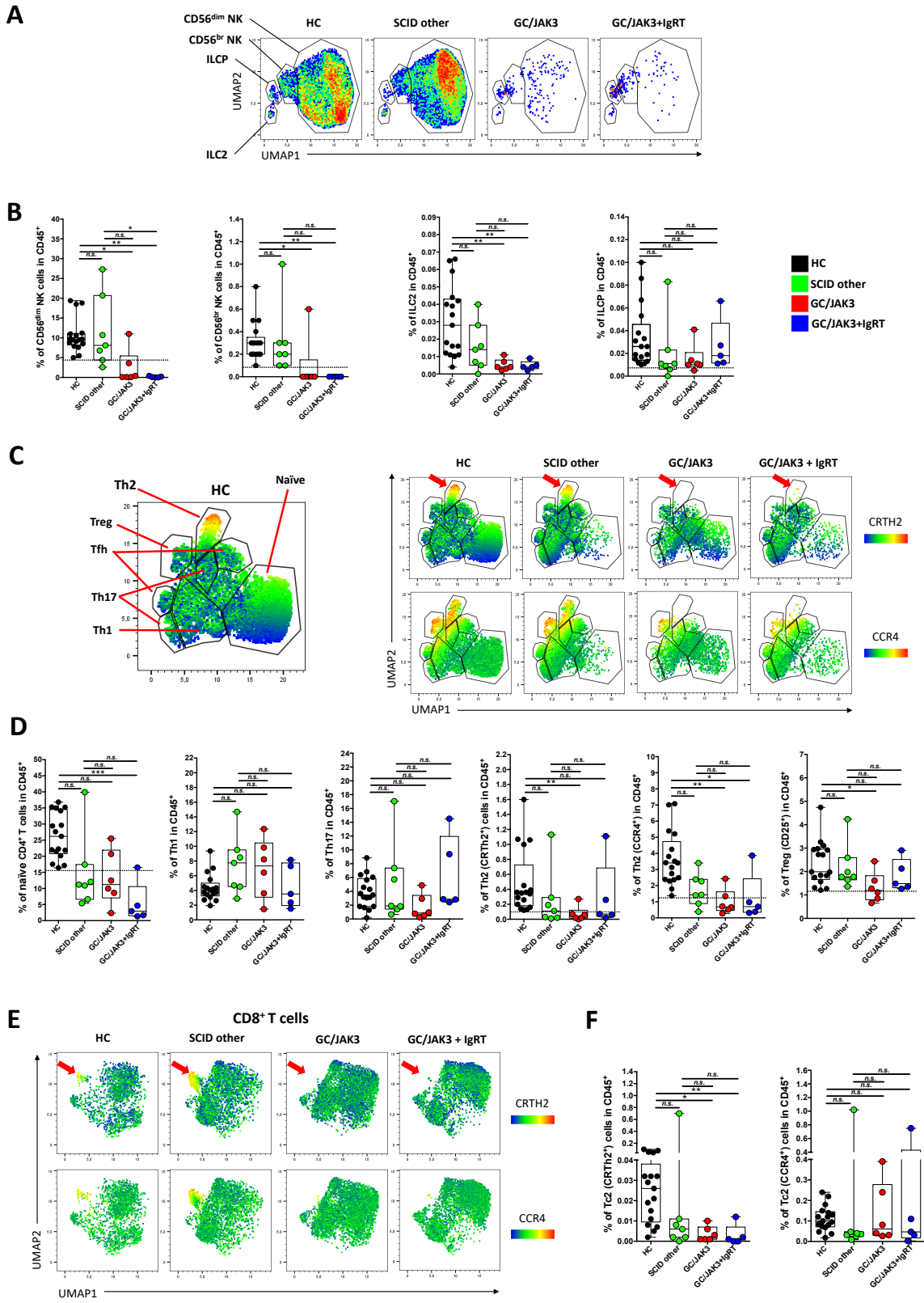


Figure 2

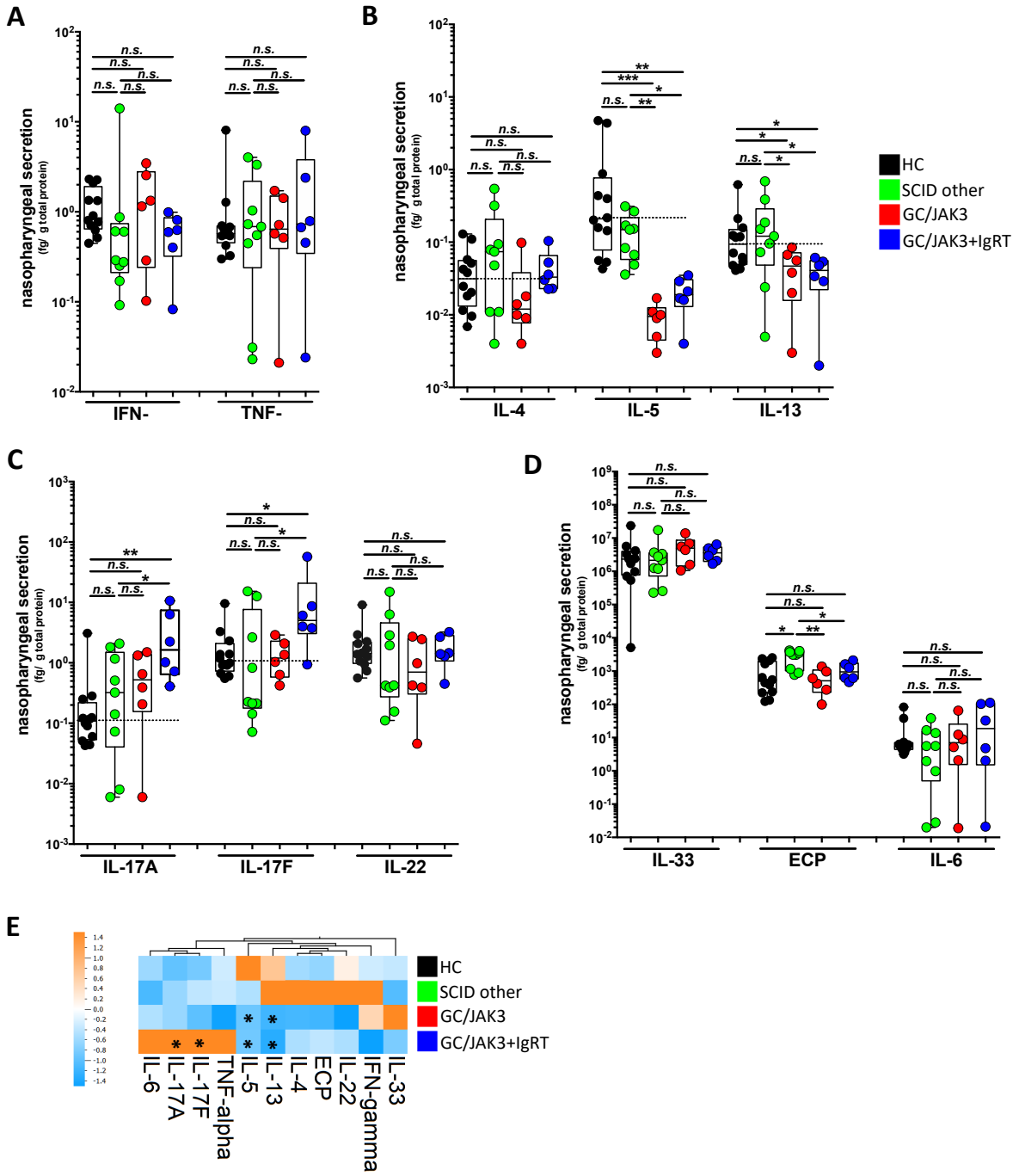


Figure 3

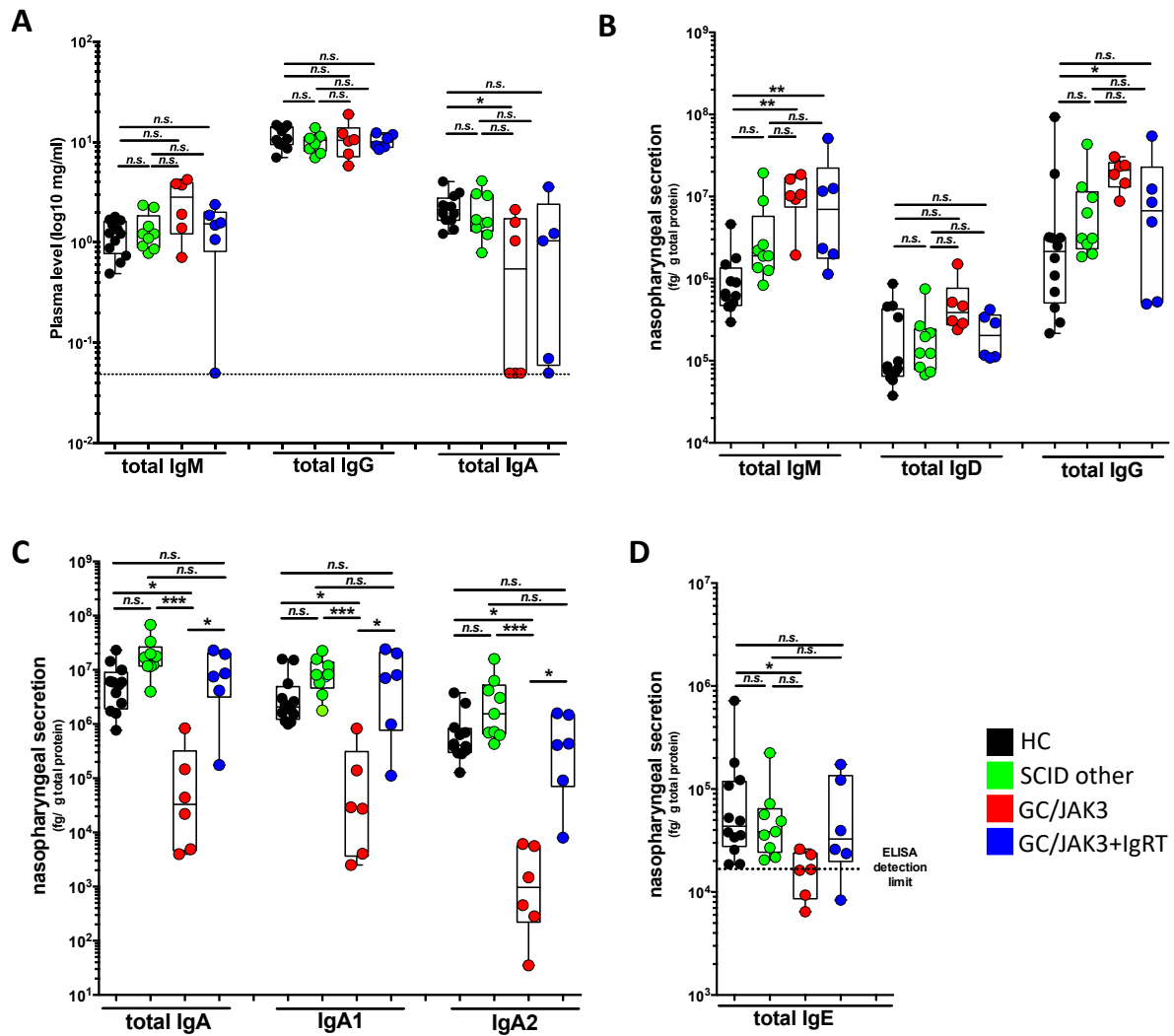




Figure 4

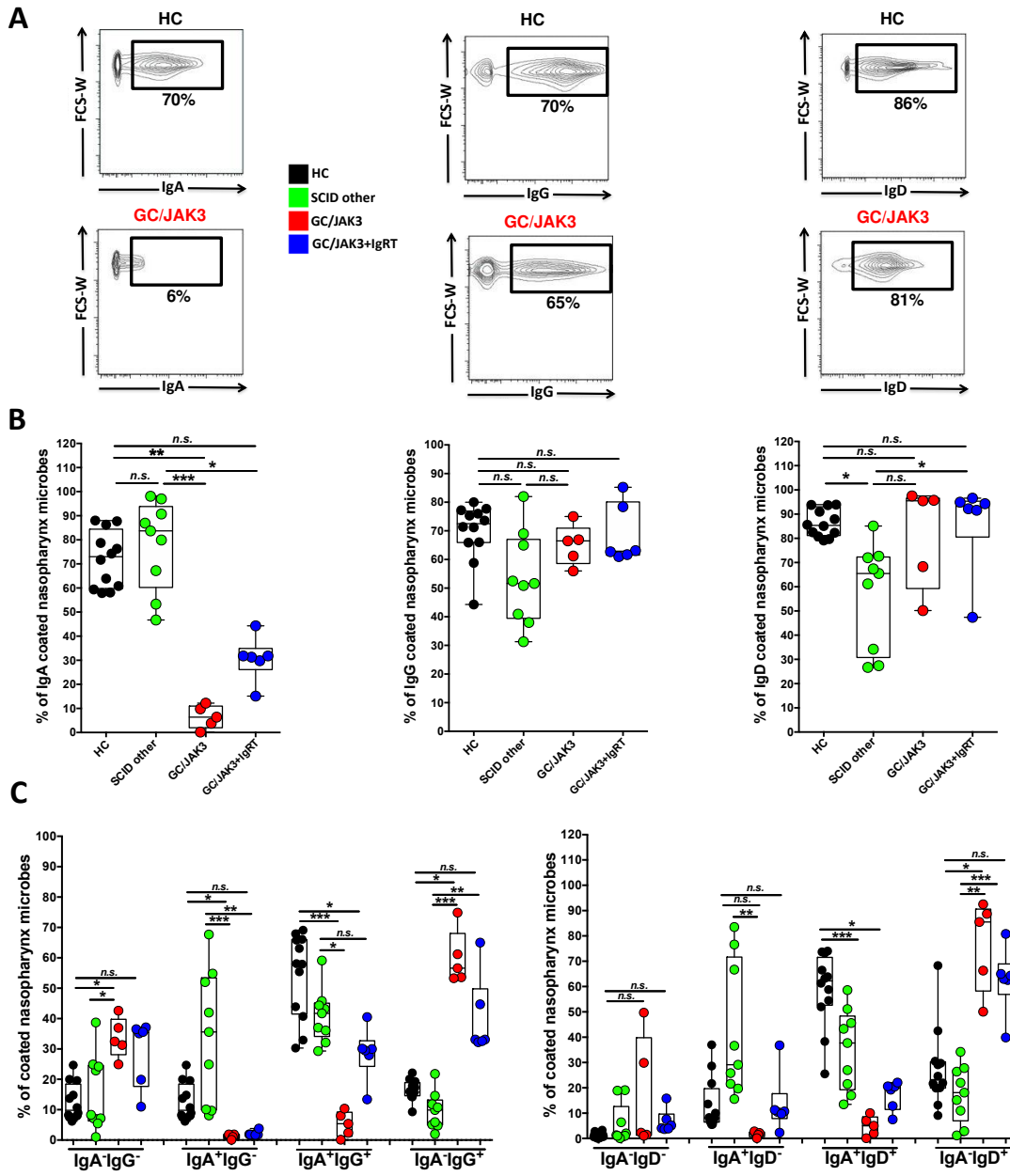


Figure 5

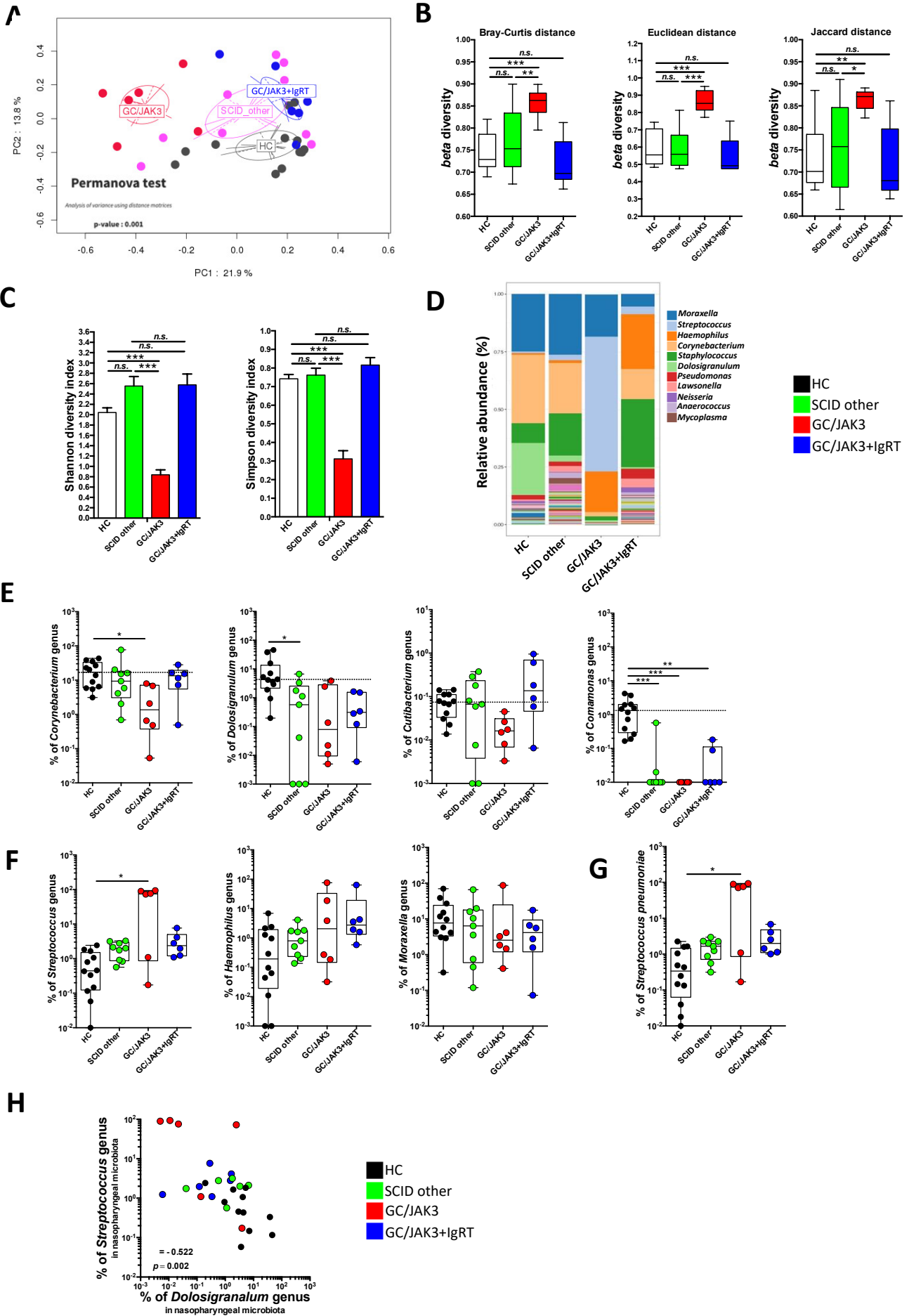


Figure 6

